Nano Biomed Eng
2018, 10(4): 406-416. doi: 10.5101/nbe.v10i4.p406-416.

Research Article

Preparation of Cu_2O Nanoparticles as a Catalyst in Photocatalyst Activity Using a Simple Electrodeposition Route

Hayder Khudhair Khattar[1], Amer Mousa Juda[1], Fouad Abdul Ameer Al-Saady[2]

[1]Department of Chemistry, Faculty of Science, University of Kufa, Najaf, Iraq.
[2]College of Pharmacy, University of Al-Mustansiriyah, Baghdad, Iraq.

Corresponding authors. E-mail: khydr12@yahoo.com; dr.fouad.a@uomustansiriyah.edu.iq

Received: Jun. 6, 2018; **Accepted:** Aug. 12, 2018; **Published:** Dec. 4, 2018.

Citation: Hayder Khudhair Khattar, Amer Mousa Juda, and Fouad Abdul Ameer Al-Saady, Preparation of Cu_2O Nanoparticles as a Catalyst in Photocatalyst Activity Using a Simple Electrodeposition Route. *Nano Biomed. Eng.*, 2018, 10(4): 406-416.
DOI: 10.5101/nbe.v10i4.p406-416.

Abstract

In order to obtain inexpensive and effective application of catalyst for photodegradation, Cu_2O powder was prepared by the simple and inexpensive electrodeposition method using surfactants such as glycerin (GLY), polyvinyl alcohol (PVA), poly(N-vinylpyrrolidone) (PVP) that helped the growth and nucleation of suspended particles. These particles were distinguished by atomic force microscopy (AFM), X-ray diffraction (XRD), field-emission scanning electron microscopy (FESEM) and high-resolution transmission electron microscopy (HRTEM). Diameter size of these obtained particles was found to reach to about 40 nm. In order to demonstrate the photodegradation efficiency of the copper oxide in the removal of organic malachite green oxalate (MG) dye, the catalyst was used both in calcination at 300 °C and without calcination. Parameters such as the amount of catalyst, the concentration of dye, the pH of dye sol, and the temperature were calculated. Pseudo first order reactions according to Langmuir-Hinshelwood kinetics could be obtained from the result of photocatalytic reactions. Parameters such as energy activation (Ea), enthalpy of activation (ΔH^0), entropy of activation (ΔS^0) and free energy of activation (ΔG^0) were calculated. The activation energy was equal to 11.719 ± 1 and 11.083 ± 1 kJ/mol for MG dye in the presence of Cu_2O nanoparticles in both two cases of calcination and without calcination respectively.

Keywords: Electrochemical deposition of Cu_2O; Photochemical processing; Thermodynamic; Kinetic; Mechanism

Introduction

Nanotechnology is in a fast progress of development and its products are quite advantageous in all domains. Nanoparticles (NPs) display a major surface-to-size proportion when they are matched to macro and micro-materials [1]. Cuprous oxide is p-type semiconductor with direct band gap of 2.0 eV, the applications of which in solar energy transmutation, gas sensors, electronics, and magnetic storage have attracted large interests [2-4]. Electrodeposition, a chemical deposition, is a method to synthesize Cu_2O nanocrystal of various shapes and sizes [5]. Properties of copper oxides have been studied through experiments and have been proven a promising photocatalyst in direct water splitting and organic contamination degradation under visible-light radiation [6, 7]. Cu_2O can adsorb molecular oxygen effectively [8], which can clean the

photogenerated electrons to inhibit the recombination of electron-hole pairs, and then develop the photocatalytic efficiency. Moreover, the essential properties of Cu_2O include low toxicity and inexpensive price [9]. Octahedral Cu_2O with bared {111} facets show extremely photocatalytic performance compared to cubes, making it a possible candidate for photocatalytic applications [10-12]. Advanced oxidation processes include the production of much interacting radicals, such as hydroxyl radicals, into least molecules, the entire mineralization of compounds into CO_2 and H_2O. The application of homogeneous photodegradation (single-phase system) to treat contaminated waters concerns the use of ultraviolet (UV)/ozone and UV/H_2O_2 [13]. Nanopwoder was characterized using atomic force microscopy (AFM), X-ray diffraction (XRD), field emission scanning electron microscope (FESEM), energy-dispersive X-ray spectroscopy (EDS), and transmission electron microscope (TEM).

Experimental

The method was simple and useful for generating NPs, which included using two electrodes, i.e. anode and cathode plates made of copper with high purity reaching to 99.99% with the scale of 2 cm, width of 2 cm and length of 1.5 mm. The two electrodes were placed facing each other in a vertical way with a distance of 6 cm between each other. The electrical cell that contained 100 mL deionized water (DW) was obtained from Faculty of Pharmacy, University of Kufa, Iraq. The electrolysis was employed at the temperature of 60 °C with continuous various voltages. The current passing in the circuit was monitored with a voltmeter. Additionally, the NPs were produced in a way of electrochemical reduction in changing the polarity of the direct current between the electrodes during electrolysis process, in order to obtain the better precipitation [14]. Electrolyte was used to prepare copper (I) oxide, with 25 g/100 mL NaCl (99% Thomas, Indi) at pH 8, and the distance for tow electrodes was 6 cm. A power supply under study (current DC 5 amp, maximum voltage 30 V, China) was utilized to supply and measure with more precision the current. Additives included glycerin (GLY), polyvinyl alcohol (PVA) and poly(N-vinylpyrrolidone) (PVP) (CDH-India). All the materials are listed in Table 1. Afterwards, the orange or red color of copper oxide powder was washed repeatedly with deionized water numerous times by using centrifugal; then washed twice with 99% ethanol and dried in an oven at 60 °C for 1h. Later, the deposited Cu_2O was stored in tightly blocked vials, in a vacuum container containing silica gel powder [15].

Result and Discussion

Characterization of Cu_2O

Atomic force microscopy (AFM) measurements of Cu_2O powder electrodeposition

AFM (CSPM-4000 Hitachi, Japan) of the Cu_2O powder was prepared by electrical method using glycerin, PVA and PVP (20 mL) as stabilizer (Fig. 1, Table 2). Fig. 1(a) shows distance among the metal

Table 1 Chemicals and working conditions applied in the experiment of Cu_2O powder electrodeposition of NaCl solutions

Chemicals		PVP	PVA	Glycerin
NaCl	25 g / 100 mL	25 g / 100 mL	25 g / 100 mL	25 g / 100 mL
NaOH	5 g / 100 mL	1.5 mL	1.5 mL	1.5 mL
$K_2Cr_2O_7$	1 g / 100 mL	1 mL	1 mL	1 mL
Citric acid	5 g / 100 mL	1 mL	1 mL	1 mL
Deionized water	0.7 μs/cm	0.7 μs/cm	0.7 μs/cm	0.7 μs/cm
Glycerin	1 g/100 mL	--	--	20 mL
PVA	1 g/100 mL	--	20 mL	--
PVP	1 g/100 mL	20 mL	--	--
pH	8-9	8-9	8-9	8-9
Temperature	50-60 ℃	50-60 ℃	50-60 ℃	50-60 ℃
General current density	500 A/m^2	500 A/m^2	500 A/m^2	500 A/m^2
(Copper) Anode area	8 cm^2	8 cm^2	8 cm^2	8 cm^2
Current density	0.4 A	0.4 A	0.4 A	0.4 A
Voltage / Time	--	3.4 V / 60 min	3.5 V / 60 min	3.8 V / 60 min

Note: PVP = Poly(N-vinylpyrrolidone); PVA = Polyvinyl alcohol.

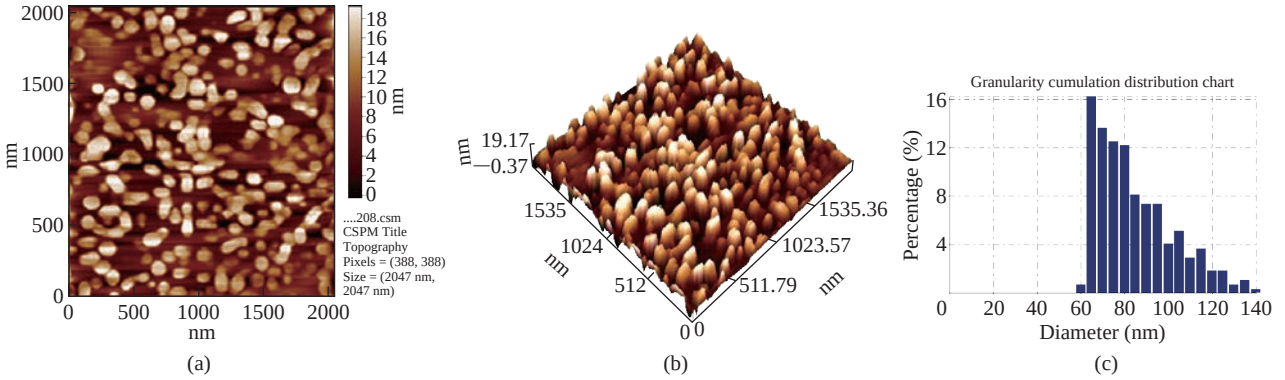

(a) (b) (c)

Fig. 1 AFM images of Cu_2O powder electrodeposition in NaCl solutions with PVP (20 mL), avg. diameter = 82.10 nm: **(a)** 2-Dimensional image; **(b)** 3-Dimensinal image; **(c)** Granulite cubulation distribution chart.

oxide NPs was equal to 18 nm; Fig. 2(b) shows distribution of the metal oxide NPs was in three dimensions: X, Y and Z [16]. X and Y represent measurement of the area, and Z = 19.17 nm represents the height within nanoscale 0-100 nm. It could be observed that distribution of the copper oxide particles ranged from 60 to 140 nm (Fig. 1(c)). Average Granulite cubulation distribution of diameter for NPs Cu_2O, when using 20 mL PVP, was 82.10 nm. Similarly, we noted the distribution of grain formed in PVA was 77.42 nm (Fig. 2), and was 56.64 nm in glycerin (Fig. 3).

X-ray diffraction (XRD) measurements of Cu_2O powder electrodeposition

The purity and crystal phases of Cu_2O powder was tested by XRD. The XRD data came from employing a Shimadzu 6000 diffractometer equipped with Cu

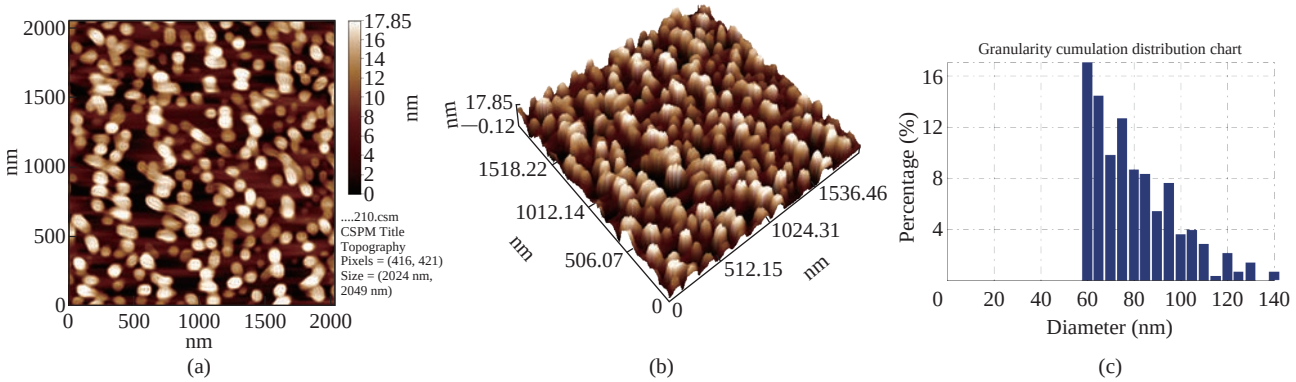

(a) (b) (c)

Fig. 2 AFM images of Cu_2O powder electrodeposition in NaCl solutions with PVA (20 mL), avg. diameter = 77.42 nm: **(a)** 2-Dimensional image; **(b)** 3-Dimensinal image; **(c)** Granulite cubulation distribution chart.

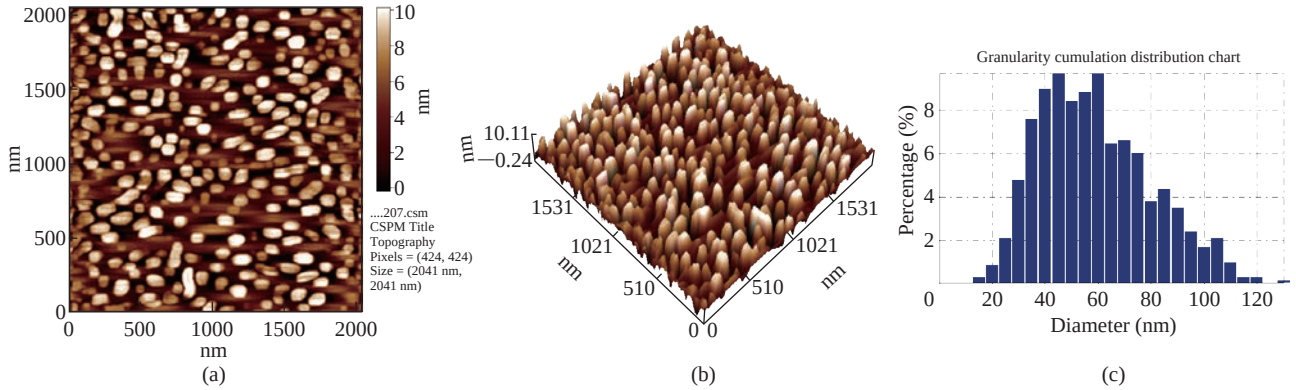

(a) (b) (c)

Fig. 3 AFM images of Cu_2O powder electrodeposition in NaCl solutions with glycerin (20 mL), avg. diameter = 56.64 nm: **(a)** 2-Dimensional image; **(b)** 3-Dimensinal image; **(c)** Granulite cubulation distribution chart.

Table 2 AFM measurements of Cu_2O powder electrodeposition in NaCl solutions by using glycerin, PVP and PVA

CSPM Imager surface roughness analysis			
Amplitude parameters			
Cu_2O	PVP	PVA	GLY
Roughness average (sa) (nm)	4.0100	4.5300	2.5900
Root mean square (sq) (nm)	4.7600	5.2100	2.9900
Surface skewness (Ssk) (nm)	0.1050	0.0672	0.0001
Surface kurtosis (sku) (nm)	2.1000	1.7900	1.8000
Sku = (3) mesokurtic, < (3) liptokurtic, > (3) platykurtic	2.1000 >	1.8000 >	1.7900
Peak-peak (sy) (nm)	19.5000	18.000	10.300
Ten point height (sz) (nm)	19.5000	18.000	10.300
Hybrid parameters			
Mean summit curvature (Ssc) (1/nm)	-0.01730	-0.0135	-0.0105
Root mean square slope (sdq) (1/nm)	0.2950	0.2670	0.2370
Surface area ratio (sdr)	3.9200	3.4400	2.6600
Functional parameters			
Surface bearing index (sbi)	2.1300	5.3000	5.5800
Core fluid retention index (sci)	1.5600	1.5100	1.4900
valley fluid retention index (svi)	0.0836	0.0700	0.0692
Reduced summit height (spk) (nm)	2.3600	2.7100	1.1000
Core roughness depth (sk) (nm)	14.3000	14.700	9.0000
Reduced valley depth (svk) (nm)	2.7800	0.5910	0.2630
Spatial parameters			
Density of summits (Sds) (1/um^2)	250.00	363.00	308.00
Fractal dimension	2.4400	2.1100	2.5200
Avg. diameter (nm)	82.10	77.42	56.64
Voltaic (V)	3.4	3.5	3.8

Kα ray (λ = 1.5406 Å) (at 40 mA and 50 KV) in zone 2θ from 20° to 80°. XRD patterns of the as-prepared samples were revealed in different conditions. In Fig. 4, diffraction peaks showed at 29.61°, 36.48°, 42.38°, 61.46°, 73.56° and 77.52°, identical to 110, 111, 200, 220, 311 and 222 planes of Cu_2O, respectively, which indicated the formation of Cu_2O nanocrystals according to JCPDS Card No. 05-0667 [17, 18]. The

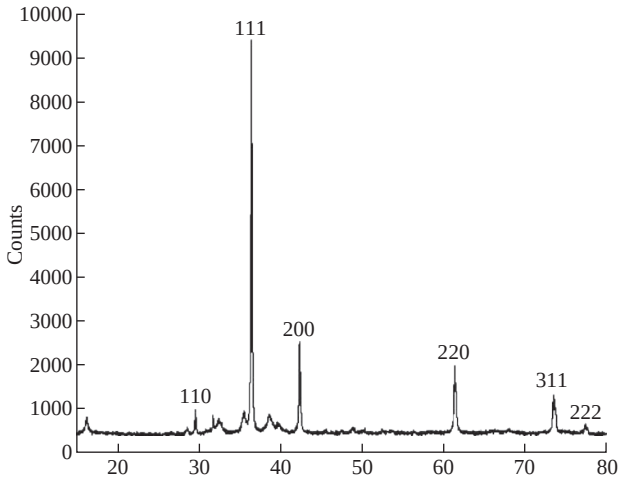

Fig. 4 X-ray images of Cu_2O powder electrodeposition in NaCl solutions.

average crystalline size of Cu_2O NPs was determined by taking the full width at half maximum (FWHM) of the most intense peak at 36.50° using Debye-Scherrer's formula, which was of about 46.50 nm. The crystalline size calculated from XRD patterns was usually bigger than that from TEM images, which also occurred in our previous study [19].

Scanning electron microscope (SEM) measurements of Cu_2O (NPs) electrodeposition with Gly, PVA, PVP

Field emission scanning electron microscopy (FESEM) (TESCAN, MIRA3, Czech) images (Fig. 5-7) show that range of the particle size of Cu_2O NPs was 40-80 nm. The TEM form revealed that the prepared Cu_2O NPs were particularly single crystals with twin boundaries (amorphous), as shown in Fig. 5. With the stabilizing agent GLY, it was found that the content of Cu in the Cu_2O NPs was 86.72 w%, and with PVA it was 83.19 w%, and with PVP it was 71.44 w%.

When the concentration of sample in glycerin (20 mL) was 1 g/100 mL, octahedral Cu_2O crystals were formed, SEM image showing the structure of Cu_2O octahedron revealed the typical morphology of octahedral Cu_2O (eight {111} faces) with about 40 nm in size (Fig. 5) [20].

TEM images from Philips CM300 300 kV High-Resolution Transmission Electron Microscope revealed the formation of octahedral Cu_2O crystals, which was compatible with the results of XRD and SEM showing particles of eight {111} faces [21] (Fig. 5).

When the sample with PVA (20 mL) was at the concentration of 1 g/100 mL, hexapods Cu_2O particles were formed with about 60 nm in size. It had eight and twenty-four {111} faces (Fig. 6).

When 20 mL PVP from 1 g / 100 mL concentration was used as stabilizer, it can yield the cubic shape of Cu_2O particles (having all six {110} faces) with formed uniform surface, and regular shape with particle size of about 80 nm according to the TEM size and SEM shape in nano scale (Fig. 7).

Photodegradation of malachite green (MG) oxalate dye by Cu_2O as catalyst

In order to prove in an electrical way the potential of copper oxide as a catalyst in the destruction of organic pollutants from pigments, wastewater or textile plants, and to satisfy the increasing demand for highly efficient and inexpensive catalysts, MG

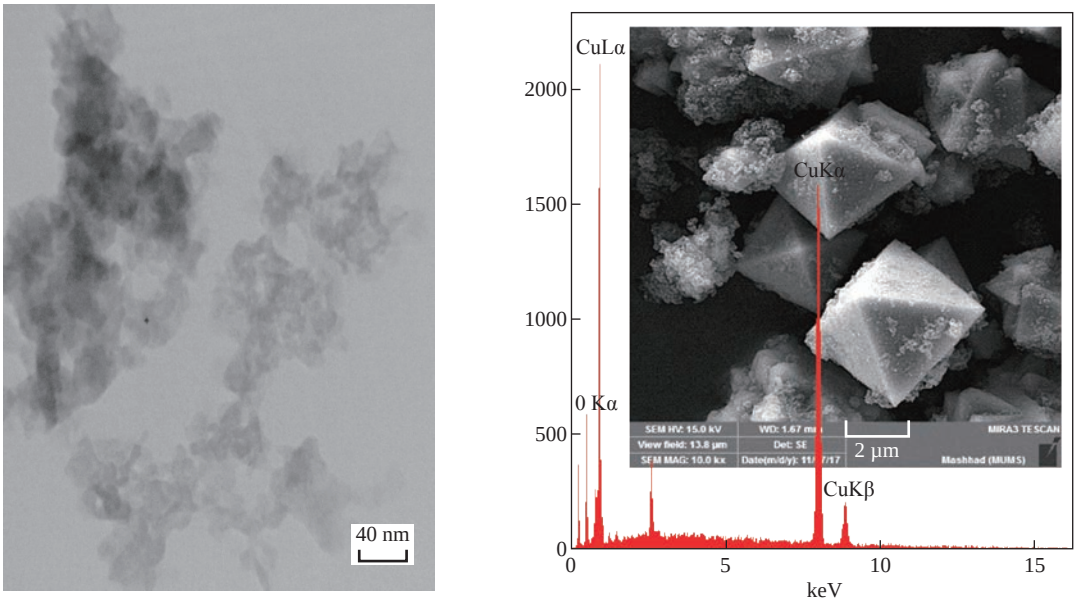

Fig. 5 SEM, EDS and TEM images of Cu_2O NPs electrodeposition in NaCl with glycerin (20 mL), size = 40 nm, under vigorous stirring. Cu = 86.72 w%, O = 13.28 w%.

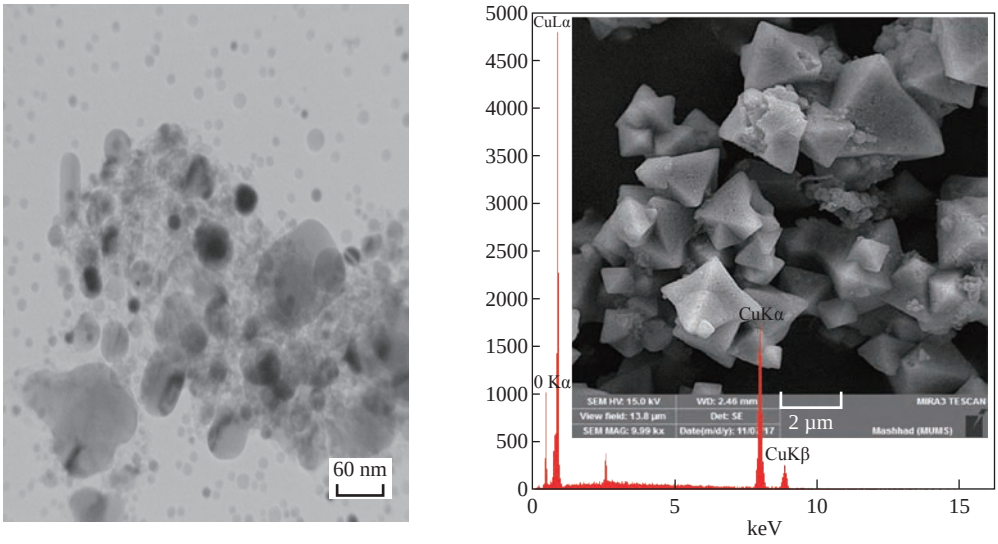

Fig. 6 SEM, EDS and TEM images of Cu_2O NPs electrodeposition in NaCl with PVA (20 mL), size = 60 nm, under vigorous stirring. Cu = 83.19 w%, O = 16.81 w%.

dye was studied with absorption of about 617 nm and good stability with visible light [22]. MG which is specific as a basic dye and a great water soluble dye related to the triphenylmethane family, M.wt 927.01 g/mol [34-36], was used to improve the photocatalytic properties. The cuprous oxide under study was used in tow phase calcined to 300 °C, termed A, and without calcination was termed B. The homely photoreactor equipment mercury lamp-Philips-Holland (250W) without cover glass as a source for UV irradiation (Shimadzu UV 1650 PC Japan) was used to determine the declination degree of the MG dye solutions (LAB Tech, Hotplate. Korea). The space of lamp and solution glass was 15 cm. The test was carried out at 25 °C, and the compartment was closed to block escape of harmful radiation. The suspension pH values were adjusted at desired level using 0.01 N NaOH or 0.01 N HCl solutions, measured via pH meter (Hanna Tool). The water mixture was stirred magnetically during the amount of dye adsorbed and reduced was determined by change in the absorbance of MG dye using Equation (1).

$$D\% = [(C_o - C_a)/C_o] \times 100\%, \quad (1)$$

where $D\%$ is the degradation ratio, C_o is the initial concentration of dye solution, and C_a is the

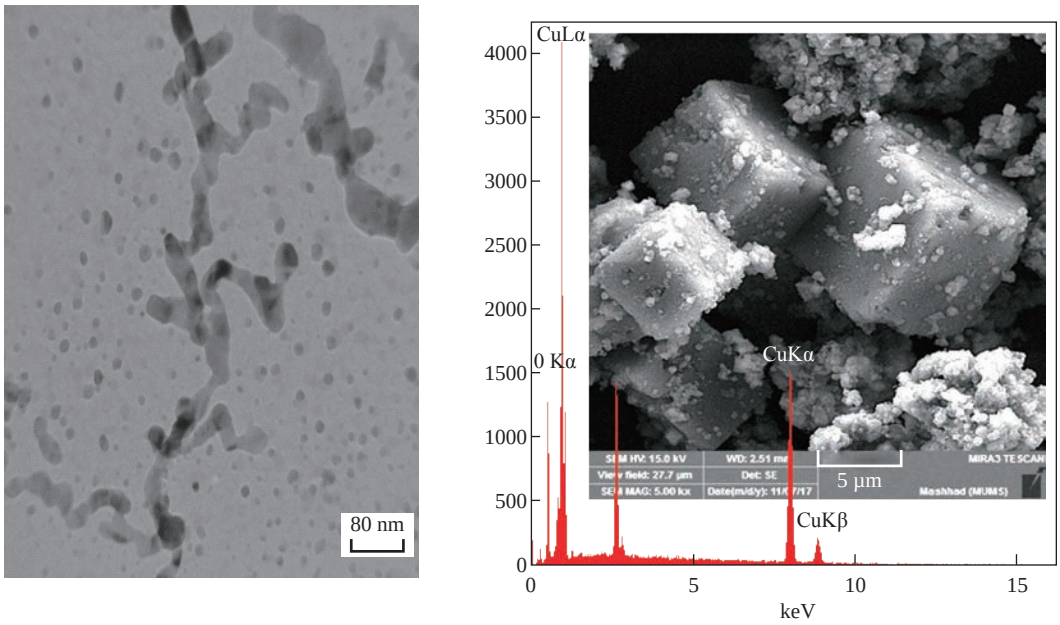

Fig. 7 SEM, EDS and TEM images of Cu_2O NPs electrodeposition in NaCl with PVP (20 mL), size = 80 nm, under vigorous stirring. Cu = 71.44 w%, O = 28.56 w%.

concentration of dyes after adsorption by the catalyst. Copper oxide obtained by electrostatic deposition method can be used in two cases in the process of photodegradation. Cu_2O calcination at 300 °C was termed A and Cu_2O without calcination was termed B.

Dark reaction of Cu_2O catalyst in the absence of ultraviolet (UV) radiation

In dark reaction tests in the lack of UV beam, Cu_2O was employed as a catalyst, as shows in Fig. 3. The results showed no deterioration in the loss of UV, where adding stimulation generated a slight change in the dye concentration. In an incubation time, the pigment concentration decreased slightly; after a limited period of time, it became fixed, where the monolayer configured on the surface of the catalyst, because of no active sites useful for extra adsorption. Hence, no additional lessening in dye concentrations was observed. Thus, the yield obtained from the tested absorption confirmed the low concentration of solutions (MG) which was due to the absorption of dyes over catalysts, and then no degradation of dyes was found. The conclusion showed that the balance occurred after 120 min. The percentage of decomposition efficiency was calculated at 76.825% and 78.185% for the Cu_2O (A and B), respectively.

Photodegradation of malachite green (MG) oxalate dye solution by ultraviolet (UV) irradiation in the absence of catalyst

Results of the photodegradation of MG dye solution, by UV irradiation in catalyst absence (Fig. 9) could be determined after 90 min of UV treating. The photodegradation efficiency (PDE%) could be observed as of 49.75% with ultraviolet radiation in catalyst absence.

Influence of the amount of catalyst

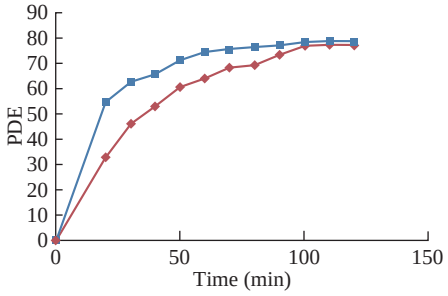

Fig. 8 The degradation efficiency of MG with A and B catalysts, in the absence of UV radiation.

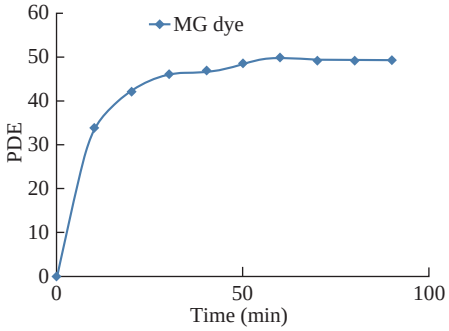

Fig. 9 The photodegradation efficiency of MG dyes without the catalyst.

Influence of the amount of catalyst onto photocatalytic degradation for MG dyes was studied. The solution was examined under the exam provision with dye concentration of 4 ppm, light power 250 W, at 25 °C and variable of the mass of Cu_2O NPs for both A and B in the range of 0.01-0.07 g in 100 mL. From 4 ppm of MG dye, if concentration of the photocatalyst crossed certain optimum value in the suspension, the penetration of light through the suspension reduced, causing decrease in the rate of decolourization of dye. Some studies explained that the rate of disintegration of the pollutant when increasing the amount of optical catalyst to the loss of a semiconductor molecule excited the state when it collided with other molecules that were not excited according to Equation (2) [23]. Thus, for executing any continuous research, the catalyst dose optimization is required before starting any photolysis process. In Fig. 10, for both copper oxides A and B, the best weight of Cu_2O was 0.03, and 0.07 g for A and B respectively. PDE for Cu_2O NPs both A and B was equal to 95.55% and 98.02% respectively.

$$TiO_2 + TiO_2 * + TiO_2 \# \rightarrow TiO_2. \quad (2)$$

The influence of pH solution

By studying the changes in pH solution in the range of 2-10 while maintaining other test conditions fixed: dye concentration of 4 ppm, light power of 250 W,

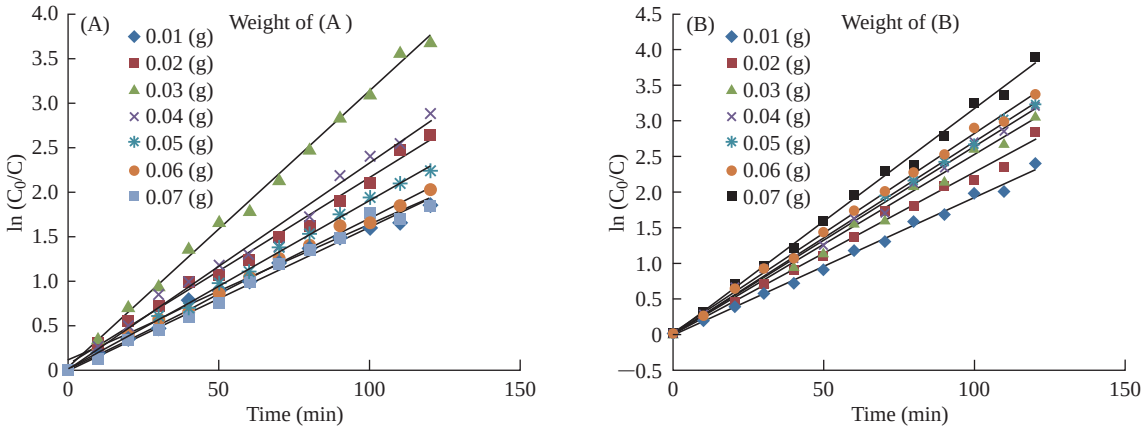

Fig. 10 **(a)** Effect of weight of Cu_2O (A) on photodegradation efficiency of MG; **(b)** Effect of weight Cu_2O (B) on photodegradation efficiency of MG.

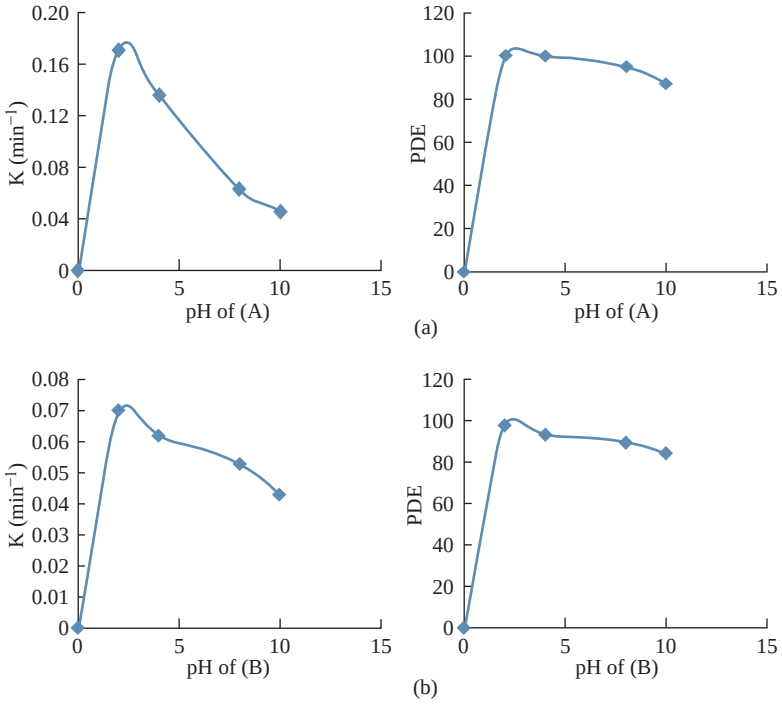

Fig. 11 Influence of pH on photocatalytic declination efficiency of MG **(a)** in the presence of 0.03 g Cu_2O (A), and **(b)** in the presence of 0.07 g Cu_2O (B).

catalyst dose of 0.03 g for sample A, and 0.07 g for sample B, at 25 °C, the chamber had a variable pH initial solution for dye solutions. The results were observed in Fig. 3 and 11; the influence of the initial solution pH on the removal of MG by Cu_2O NPs were shown. It can be seen that the adsorption percentage maintained very high, as of 99.97 and 97.53% for both cuprous oxides A and B respectively, in the pH range of 2-8. And then, the adsorption of MG decreased gradually from 94.85 and 89.71% to 87.09 and 84.34% for both cuprous oxides A and B respectively.

Influence of primary dye concentration

The influence of primary dye concentration on the photocatalytic degradation rate could be calculated by maintaining all other test conditions stable: light power = 250 W, pH = 2 at 25 °C, 0.03 g for Cu_2O (A) and 0.07 g for Cu_2O (B), while changing the primary dye concentration in the domain of 1-7 ppm. Fig. 12 shows that the photocatalytic degradation rate was elevated

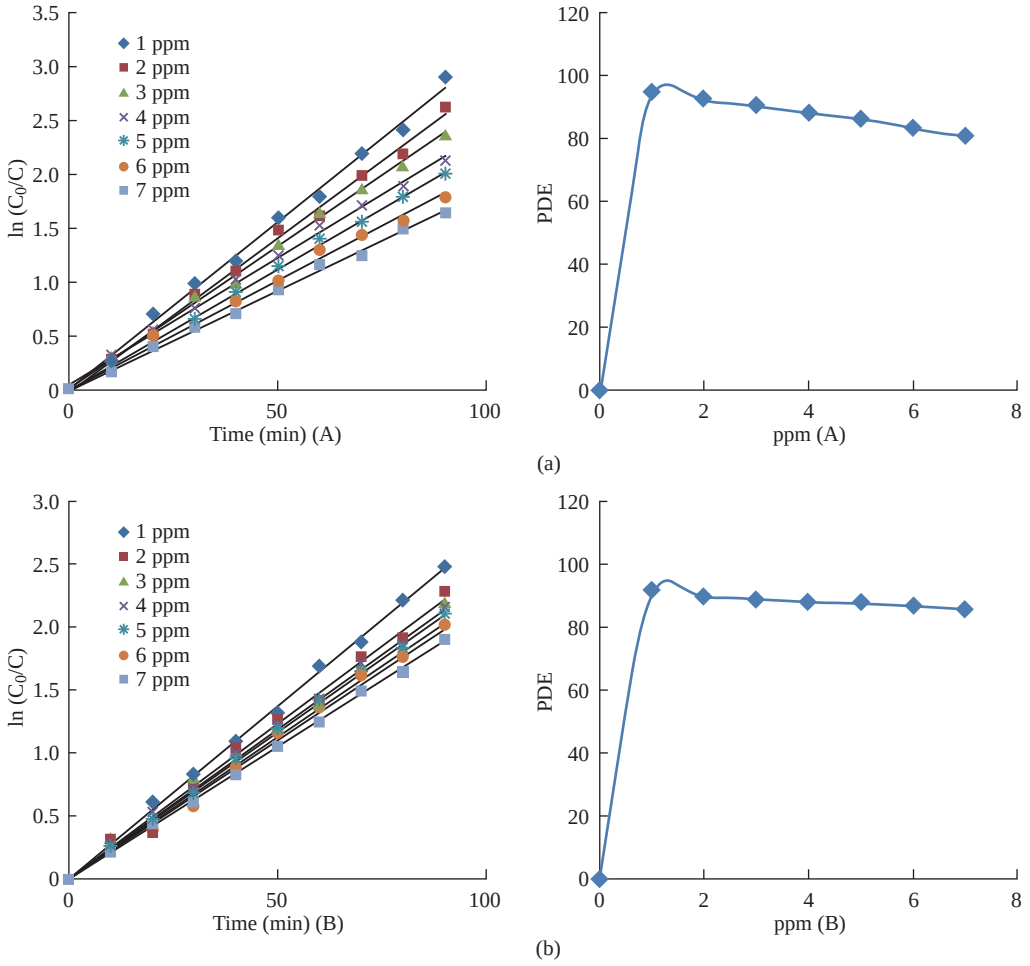

Fig. 12 The variable in photocatalytic degradation efficiency for MG dye with concentration **(a)** in the presence of 0.03 g Cu_2O (A), and **(b)** in the presence of 0.07 g Cu_2O (B).

Table 3 Values of rate constant, kinetics and thermodynamic parameters for the photocatalytic degradation of MG dye at 303-318 K, with 0.03 g Cu_2O (A) and 0.07 g Cu_2O (B)

T(k°)	1/T	K(sec^{-1}) ×10^{-5}		ln K		Ea (kJ mol^{-1})		$\Delta H^{\#}$ (kJ mol^{-1})		$\Delta S^{\#}$ (kJ mol^{-1} k^{-1})		$\Delta G^{\#}$ (kJ mol^{-1})	
		Cu_2O (B)	Cu_2O (A)	Cu_2O (B)	Cu_2O (A)	Cu_2O (B)	Cu_2O (A)	Cu_2O (B)	Cu_2O (A)	Cu_2O (B)	Cu_2O (A)	Cu_2O (B)	Cu_2O (A)
303	0.00330	4.166	5.833	-10.085	-9.749			8.564	9.200			84.495	95.850
308	0.00324	4.660	6.698	-9.973	-9.611			8.522	9.158			85.706	97.246
						11.083	11.719			-0.250	-0.286		
313	0.00319	5.166	7.329	-9.870	-9.521			8.481	9.117			86.918	98.635
318	0.00314	5.500	7.833	-9.808	-9.454			8.439	9.075			88.129	100.023

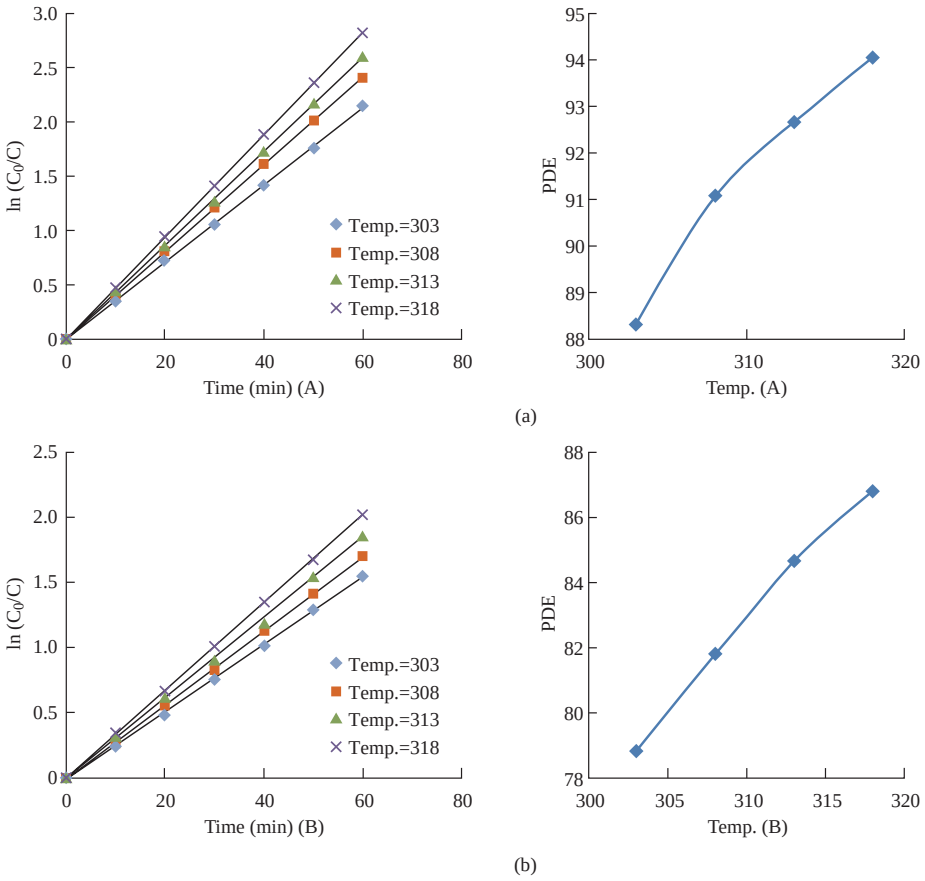

Fig. 13 Influence of photocatalytic degradation efficiency of MG at varied temperature **(a)** in the presence 0.03 g Cu_2O (A), and **(b)** in the presence of 0.07 Cu_2O (B).

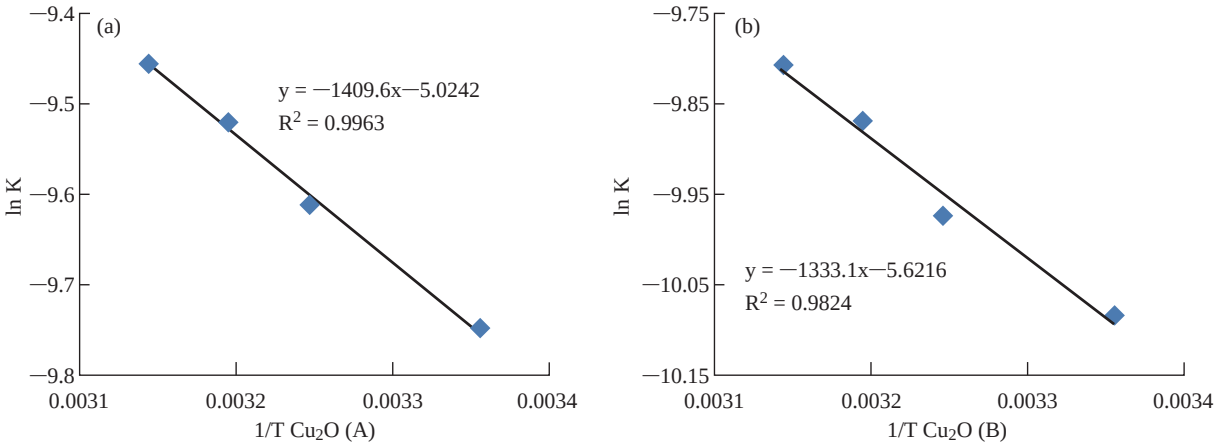

Fig. 14 Arrhenius plot of MG dye with **(a)** 0.03 g Cu_2O (A) and **(b)** 0.07 g Cu_2O (B).

with lowering of the initial dye concentration. This might be due to the length of the path of photon entering the dye solution that decreased with the increased concentration of the dye solution, which resulted in a fewer number of photons attached to the surface of the catalyst, Thus, the hydroxyl root (OH) and the superoxide (O^{2-}) were lowering, leading to a reduction in the percentage of photolysis due to the lack of surface area exposed to excitement [24, 25].

Influence of varied temperature

Table 3 shows the activation energy for photocatalytic degradation in MG solution using the cuprous oxide: 0.03 g Cu_2O (A) and 0.07 g Cu_2O (B). The catalyst in the temperature range of 303-318 K equaled 11.719 ± 1 and 11.083 ± 1 kJ/M, respectively.

Conclusions

The preparation of cuprous oxide NPs was carried out successfully by electrochemical rout, in an easy, inexpensive and highly precise manner to control the size and shape within nanometer scale. The prepared NPs were characterized by XRD, FESEM, EDX, TEM and AFM. To improve the catalytic performance of photodegradation and to enhance crystallization, the powder was calcined to 300 °C (A), To test the catalytic performance, Cu_2O calcination was compared with Cu_2O without calcination (B). For degradation of the sol malachite green dye, the product photocatalytic reactions suggested that the model was pseudo-first order reaction represented by the Langmuir-Hinshelwood model. The thermodynamic parameters referred to that positive ΔH^0 was certain on endothermic reaction. The positive ΔG^0 result indicated that the non-spontaneous reaction was of clear high positive ΔG^0, which was because the activated case was solvated structure established between the dye molecules and the reaction mediate that was hydroxyl radicals. This was also confirmed by the negative entropy of activation ΔS^0 which was negative and more ordered to the reactant. The reactive species such as hydroxyl radical and superoxide anion were produced from the heterogeneous photocatalytic reaction. The products of the fragmentation of the dye by the catalyst were CO_2 and H_2O. Future work should be the production of low-cost semiconductors capable of eliminating organic pollutants in an easy, simple and controlled electrochemical way.

Conflict of Interests

The authors declare that no competing interest exists.

References

[1] K.V. Abhinav, R.V.K. Rao, P.S. Karthik, et al., Copper conductive inks: synthesis and utilization in flexible electronics. *RSC Advances*, 2015, 5(79): 63985-64030.

[2] R.N. Briskman, A study of electrodeposited cuprous oxide photovoltaic cells. *Sol. Energy Mater. Sol. Cells*, 1992, 27: 361-368.

[3] J. Zhang, J. Liu, Q. Peng, et al., Nearly monodisperse Cu_2O and CuO nanospheres: Preparation and applications for sensitive gas sensors. *Chem. Mater*, 2006, 18: 867-871.

[4] P. Poizot, S. Laruelle, S. Grugeon, et al., Nano-sized transition-metaloxidesas negative-electrode materials for lithium-ion batteries. *Nature*, 2000, 407: 496-499.

[5] L. Xiangfeng, Z. Ruimin, S. Xiaohai, et al., Cu_2O nanoparticles: Radiation synthesis, and photocatalytic activity. *Nucl. Sci. Tech.*, 2010, 21: 146-151.

[6] M. Hara, T. Kondo, M. Komoda, et al., Cu_2O as a photocatalyst for overall water splitting under visible light irradiation. *Chem. Commun.*, 1998, 2(3): 357-358.

[7] Y.G. Zhang, L.L. Ma, J.L. Li, et al., In situ fenton reagent generated from TiO_2/Cu_2O composite film: A new way to utilize TiO2 under visible light irradiation. *Environ. Sci. Technol*, 2007, 41: 6264-6269.

[8] J. Li, L. Li, Y. Yu, et al., Preparation of highly photocatalytic active nano-size TiO_2–Cu_2O particle composites with a novel electrochemical method. *Electrochem. Commun.*, 2004, 6: 940-943.

[9] W. Siripala, A. Ivanovskaya, T.F. Jaramillo, et al., A Cu_2O=TiO_2 heterojunction thin film cathode for photoelectrocatalysis. Sol. Energy Mater. Sol. *Cells*, 2003, 77: 229-237.

[10] X.Q. Gong, A.J. Selloni, Reactivity of anatase TiO_2 nanoparticles: The role of the minority (001) surface. *Phys. Chem. B*, 2005, 109: 19560-19562.

[11] X.G. Han, Q. Kuang, M.S. Jin, et al., Synthesis of titania nanosheets with a high percentage of exposed (001) facets and related photocatalytic properties. *J. Am. Chem. Soc.*, 2009, 131: 3152-3153.

[12] H. Xu, W. Wang, and W. Zhu, Shape evolution and size-controllable synthesis of Cu_2O octahedra and their morphology-dependent photocatalytic properties. *J. Phys. Chem. B*, 2006, 110: 13829-13834.

[13] A. Verma, Advanced oxidation technologies for wastewater treatment. Proceedings of the M. Tech Seminar, 2004.

[14] M. Raposo, Q. Ferreira, and P.A. Ribeiro, A guide for atomic force microscopy analysis of soft condensed matter. *Modern Research and Educational Topics in Microscopy*. Formatex, 2007, 758-769.

[15] M.M.A. Shirazi, Characterization of electrospun polystyrene membrane for treatment of biodiesel's water-washing effluent using atomic force microscopy. *Desalination*, 2013, 329: 1-8.

[16] E.S. Gadelmawla, M.M. Koura, T.M.A. Maksoud, et al., Roughness parameters. *J. Mater. Process. Technol.*, 2002, 123: 133-145.

[17] K. Giannousi, G. Sarafidis, S. Mourdikoudis, et al., Selective synthesis of Cu_2O and Cu/Cu_2O NPs: antifungal activity to yeast saccharomyces cerevisiae and DNA interaction. *Inorganic Chemistry*, 2014, 18(53): 9657-9666.

[18] A. Khan, A. Rashid, R. Younas, et al., A chemical reduction approach to the synthesis of copper nanoparticles. *International Nano Letters*, 2016, 1(6): 21-26.

[19] A.Q. Le, V.P. Dang, N.D. Nguyen, et al., Preparation of polypropylene/silver nano-zeolite plastics and evaluation of antibacterial and mechanical properties. *International Journal of Composite Materials*, 2016, 4(6): 89-94.

[20] L. Feng, C. Zhang, G. Gao, et al., Facile synthesis of hollow Cu_2O octahedral and spherical nanocrystals and their morphology-dependent photocatalytic properties. *Nanoscale Res. Lett.*, 2012, 1(7): 276.

[21] Y. Won, L.A. Stanciu, W. Lafayette, et al., Cu_2O and Au/Cu_2O particles: surface properties and applications in glucose sensing. *Sensors*, 2012, 12: 13019-13033.

[22] W. Jiang, X. Wang, Z. Wu, et al., Silver oxide as superb and stable photocatalyst under visible and near-infrared light irradiation and its photocatalytic mechanism. *Ind. Eng. Chem. Res*, 2015, 3(54): 832-841.

[23] O.E. Kartal, M. Erol, and H. Oguz, Photocatalytic destruction of phenol by TiO_2 powders. *Chemical Engineering & Technology*, 2001, 24(6): 645-649.

[24] K. Hustert, R.G. Zepp, Photocatalytic degradation of selected azo dyes. *Chemosphere*, 1992, 3(24): 335-342.
[25] N. Daneshvar, S. Aber, and F. Hosseiazadeh, Study of C.I. acid orange 7 removal in contaminated water by photooxidation processes. *Global NEST Journal*, 2008, 1(10): 16-23.